STELLAR VELOCITY DISPERSION OF THE LEO A DWARF GALAXY

Warren R. Brown, Margaret J. Geller, Scott J. Kenyon, Michael J. Kurtz

Smithsonian Astrophysical Observatory, 60 Garden St, Cambridge, MA 02138

Accepted in ApJ

ABSTRACT

We measure the first stellar velocity dispersion of the Leo A dwarf galaxy, $\sigma = 9.3 \pm 1.3$ km s^{-1}. We derive the velocity dispersion from the radial velocities of ten young B supergiants and two HII regions in the central region of Leo A. We estimate a projected mass of $8 \pm 2.7 \times 10^7$ $M_\odot$ within a radius of $2'$, and a mass to light ratio of at least 20 ± 6 $M_\odot/L_\odot$. These results imply Leo A is at least $\sim 80\%$ dark matter by mass.

Subject headings: galaxies: individual (Leo A)

<div style="columns:2">

1. INTRODUCTION

The Leo A dwarf galaxy was discovered by Zwicky (1942) and is one of the most remote galaxies in the Local Group. Leo A is gas rich, with an H I velocity dispersion of 3.5 to 9 km s^{-1} and with no observed rotation (Allsopp 1978; Lo et al. 1993; Young & Lo 1996). Leo A is also extremely metal poor, with an abundance of $12 + \log O/H = 7.3$ to 7.4 measured from H II regions (Skillman et al. 1989; van Zee et al. 2006).

Photometric studies of Leo A reveal both a red and blue plume of stars in its color-magnitude diagram indicating recent star formation (Demers et al. 1984; Sandage 1986; Tolstoy 1996). *Hubble Space Telescope* observations have resolved the stellar population of Leo A, which shows evidence for numerous epochs of star formation spanning billions of years (Tolstoy et al. 1998; Schulte-Ladbeck et al. 2002; Cole et al. 2007) as well as an old stellar "halo" (Vansevičius et al. 2004). RR Lyrae variables confirm the presence of an ~ 11 Gyr old population, and place Leo A at a distance of 800 ± 40 kpc (Dolphin et al. 2002). Recently, Brown et al. (2006) reported the first spectroscopy of stars in Leo A: two B supergiants stars observed serendipitously as part of their hypervelocity star survey. The B supergiants provide spectroscopic proof of star formation as recently as ~ 30 Myr ago in Leo A.

Inspired by the B supergiant observations, we have obtained spectroscopy for ten additional blue-plume objects in Leo A. There is no a-priori reason to expect that Leo A's steller and H I gas velocity dispersions are identical. Detailed H I maps show velocity structure, which suggests that the gas may be affected by cooling or may not yet be relaxed (Young & Lo 1996). Our observations allow us to measure the stellar velocity dispersion, and thus estimate the mass of Leo A's dark matter halo. In §2 we discuss our target selection, observations, and stellar radial velocity determinations. In §3 we present the resulting velocity dispersion and mass-to-light ratio of Leo A. We conclude in §4.

2. DATA

2.1. *Target Selection*

We use Sloan Digital Sky Survey (SDSS, Adelman-McCarthy et al. 2007) photometry to se-

Electronic address: wbrown@cfa.harvard.edu

lect candidate Leo A blue plume stars by color. We illustrate our target selection in Figure 1, a color-color diagram of every star in SDSS Data Release 5 with $g' < 21$ and within $9'$ of Leo A (see also Figure 2). We compute de-reddened colors using extinction values obtained from Schlegel et al. (1998); the adopted extinction values are $E(u' - g') = 0.029$ and $E(g' - r') = 0.022$. Objects with $(g' - r')_0 < 0$ and $(u' - g')_0 < 1.1$ are objects in the blue plume. The blue plume can contain massive main sequence stars, blue supergiant stars, and blue-loop stars (e.g. Schulte-Ladbeck et al. 2002). We target the 12 blue plume objects with $g' < 21$ (solid squares and triangles).

Objects with $(g' - r')_0 > 0$ in Figure 1 have colors consistent with foreground stars, ranging from F-type stars at the main sequence turn-off $(g' - r')_0 \sim 0.2$ to late M dwarfs $(g' - r')_0 > 1$. Stars with $(g' - r')_0 \sim 1.4$ may include some asymptotic giant branch stars in Leo A.

Figure 2 plots the position of every star in Figure 1. For reference, the ellipses follow Leo A's observed H I profile, with center $9^h59^m23^s.92$ $+30°44'47''.69$ (J2000), semiminor to semimajor axis ratio 0.6, and position angle $104°$ (Young & Lo 1996). The solid ellipse marks Leo A's Holmberg radius $a = 3'.5$ (Mateo 1998), and the dotted ellipse with $a = 8'.0$ marks the extent of Leo A's H I gas (Young & Lo 1996) and stellar "halo" (Vansevičius et al. 2004). All twelve blue plume candidates are located within $2'$ of the center of Leo A; probable foreground objects are distributed more uniformly across the field.

2.2. *Observations*

We obtained spectroscopy of the twelve blue plume objects with the 6.5m MMT telescope and the Blue Channel spectrograph. Observations occurred during the course of our hypervelocity star survey program on the nights of 2005 Dec 5-6, 2006 May 24-25, 2006 June 20, 2006 Dec 27, and 2007 Mar 18. We operated the Blue Channel spectrograph with the 832 line mm^{-1} grating in 2nd order and with a $1.25''$ slit. These settings provided a wavelength coverage of 3650 Å to 4500 Å and a spectral resolution of 1.2 Å. One object (an H II region) was reobserved with the 300 line mm^{-1} grating and a $1''$ slit, providing wavelength coverage from 3400 Å to 8600 Å with a spectral resolution of 6.2 Å. Exposure times were 30 minutes. We obtained comparison lamp exposures af-
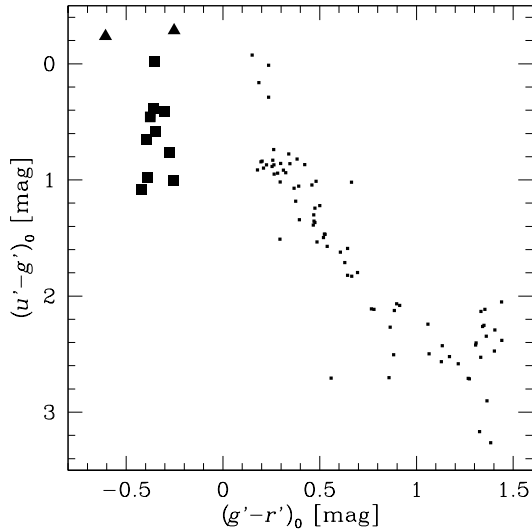
</div>

FIG. 1.— Color-color diagram of every star in SDSS with $g' < 21$ and within $9'$ of Leo A (centered at $9^h59^m23\overset{s}{.}92$ $+30°44'47\overset{''}{.}69$ J2000). We target the twelve blue plume candidates with $(g' - r')_0 < 0$. We identify ten B supergiants (*solid squares*) and two H II regions (*solid triangles*).
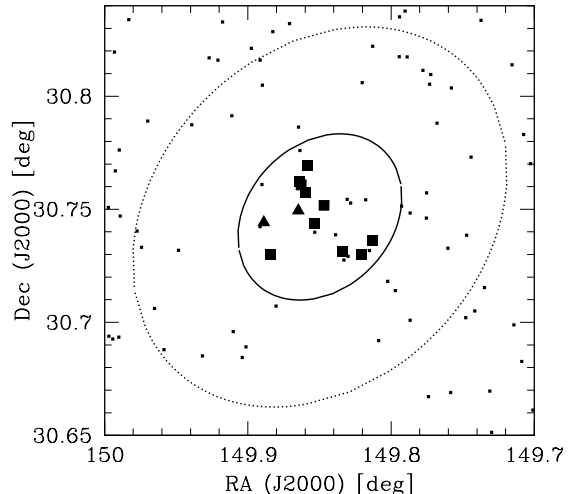

FIG. 2.— Location of objects in Figure 1, where the symbols are the same as before. For reference, the solid ellipse marks Leo A's Holmberg radius $a = 3\overset{'}{.}5$ (Mateo 1998) and the dotted ellipse marks the extent of Leo A's stellar "halo" (Vansevičius et al. 2004) and H I gas (Young & Lo 1996).

ter every exposure. The wavelength solutions are determined from 44 lines with typical root-mean-square residuals of ±0.05 Å, or ±4 km s^{-1}. We note that the single slit spectrograph is a compact instrument with minimal flexure: wavelength solutions shift by less than 1 pixel (0.355 Å) during a night, easily measured from individual comparison lamp exposures.

2.3. *Spectroscopic Identifications*

Ten blue plume objects are stars of B spectral type and two are H II regions. Figure 3 plots the spectra of the ten stars and the two H II regions, summed and shifted to the rest frame. The signal-to-noise ratios (S/N) of the individual spectra range from $S/N = 6$ to 15 per pixel at 4000 Å, and depend on target's apparent magnitude and the seeing conditions of the observation.

The ten B-type stars have visibly narrower Balmer lines and thus lower surface gravity than the other B-type stars in the Brown et al. (2006, 2007) hypervelocity star survey. Cross-correlation with MK spectral standards (Gray et al. 2003) indicates that the stars are probably luminosity class I or II B supergiants, consistent with the stars' inferred luminosities.

At the distance modulus of Leo A $(m - M)_0 = 24.51 \pm 0.12$ (Dolphin et al. 2002), the ten B-type stars have absolute magnitudes ranging from $M_V = -5.3$ to -3.4. For comparison, Corbally & Garrison (1984) give absolute magnitudes $M_V = -5.5$ for a B9 Ib star and $M_V = -3.1$ for a B9 II star. We conclude the ten stars are likely B supergiants in Leo A. Such B supergiants have ages ranging from ~30 Myr for the most luminous stars to ~200 Myr for the least luminous stars (Schaller et al. 1992).

2.4. *Radial Velocities*

We measure radial velocities with the cross-correlation package RVSAO (Kurtz & Mink 1998). We begin by observing the B9 II star γ Lyr by quickly scanning the star across the spectrograph slit. This procedure provides us with a very high signal-to-noise ratio cross-correlation template with a known velocity (Evans 1967; Gray et al. 2003). The accuracy of the velocity zero-point comes from the error on the mean of the 44 comparison lamp lines used to determine the template's wavelength solution, ±0.6 km s^{-1}.

Is is important that we maximize velocity precision for our velocity dispersion measurement, and we achieve the best precision by cross-correlating the stars with themselves. Thus, after measuring the stars' velocities with the γ Lyr template, we shift the spectra to the rest frame and sum them together to create a second template (shown in Figure 3). We then cross-correlate the ten stars with this second template of themselves. Table 1 lists the resulting heliocentric radial velocities and errors. The mean cross-correlation precision is ±3.7 km s^{-1}.

We also measure the radial velocities of the H II regions with RVSAO, but this time using Gaussian fits to the emission lines. The final velocity of SDSS J095927.532+304457.75 comes from a weighted mean of the 3727 [OII] doublet (resolved in our spectra), Hδ, and Hγ emission lines. A low-dispersion spectrum of SDSS J095933.320+304439.21 provides additional line measurements from Hβ, [OIII], and Hα for that object. The velocity of SDSS J095933.320+304439.21 is the weighted average of all of its observed lines. The mean emission-line velocity error is ±3.9 km s^{-1}.

3. RESULTS

3.1. *Stellar Velocity Dispersion*

The average velocity of our twelve Leo A objects is 22.3 ± 2.9 km s^{-1} (see Figure 4), statistically identical with the 23 ± 3 km s^{-1} systemic H I velocity measured by Allsopp (1978) and the 23.2 - 24.0 km s^{-1} systemic H I velocities measured by Young & Lo (1996). Thus the velocities of our twelve objects are all consistent with membership in Leo A.

The root-mean-square velocity dispersion of our twelve objects is 10.0 km s^{-1}. We derive the intrinsic velocity
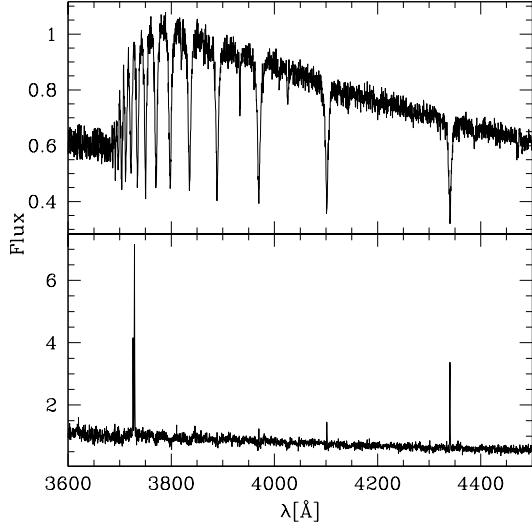
FIG. 3.— MMT spectra of the ten B supergiants (*upper panel*) and the two H II regions (*lower panel*), summed together and shifted to rest frame. The continuum fluxes are arbitrarily normalized.
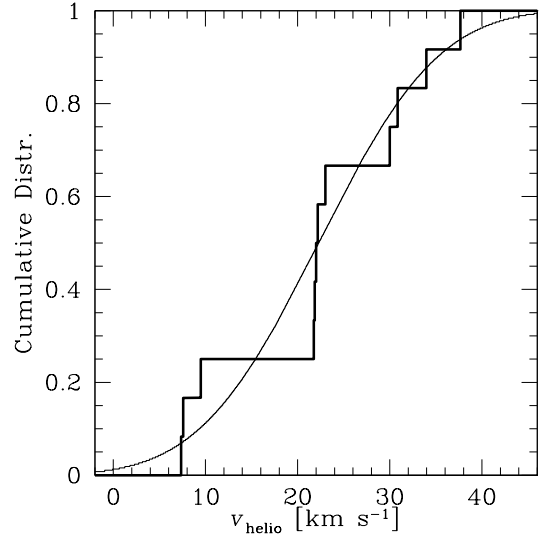

FIG. 4.— Cumulative distribution of the observed velocities (*histogram*) compared to a Gaussian distribution (*curve*) with dispersion 10.0 km s^{-1} and mean velocity 22.3 km s^{-1}.

dispersion by subtracting in quadrature the average 3.8 km s^{-1} uncertainty of the observations. Thus we measure an intrinsic stellar velocity dispersion of $\sigma = 9.3 \pm 1.3$ km s^{-1}.

We estimate the robustness of the velocity dispersion measurement by comparing the cumulative distribution of velocities to a Gaussian distribution (see Figure 4). A Kolmogorov-Smirnov test finds a 0.5 likelihood of drawing the twelve objects from a Gaussian distribution with the observed velocity dispersion. Greater number statistics are always desirable, but it appears that the twelve blue plume objects provide a statistically sound measurement of Leo A's stellar velocity dispersion.

Our stellar velocity dispersion measurement is identical to the H I gas velocity dispersion measured by Young & Lo (1996): 9.3 ± 1.4 km s^{-1}. Young & Lo (1996) also observe an H I component with 3.5 ± 1.0 km s^{-1} dispersion localized in high column-density regions. If we remove the two H II regions from our own analysis, the B-type stars have a mean velocity of 21.5 ± 3.4 km s^{-1} and an intrinsic velocity dispersion of $\sigma_B = 10.1 \pm 1.3$ km s^{-1}. This dispersion is statistically identical to our original value.

There is no evidence for rotation of the stellar component of Leo A; the high- and low-velocity blue plume objects appear inter-mixed on the sky. This result is consistent with absence of rotation seen in the H I gas (Lo et al. 1993; Young & Lo 1996). Given that detailed H I maps show velocity structure in Leo A (Young & Lo 1996), it is possible that additional observations may reveal structure in the stellar radial velocity distribution.

3.2. *Mass-to-Light Ratio*

We now estimate the kinematic mass of Leo A. Because there is no evidence for rotation, we assume that the galaxy is in pressure equilibrium and apply two simple mass estimators: the virial theorem, and the projected mass estimator of Heisler et al. (1985). The virial mass is given by $M_{vir} = 696 R_e \sigma_z^2$ $M_\odot$, where R_e is the effective radius in pc and σ_z is the one-dimensional velocity dis-

persion in km s^{-1}. Our objects are located inside a radius of $2' = 500$ pc, while Leo A's observed stellar distribution extends to a radius of $8' = 2000$ pc. If we choose $R_e = 500$ pc, Leo A's virial mass is $M_{vir} \sim 3 \times 10^7$ $M_\odot$.

The virial theorem, however, is both more biased and less stable for small numbers of test particles than is the projected mass estimator (Bahcall & Tremaine 1981). Thus we use the Heisler et al. (1985) projected mass estimator to obtain a more accurate estimate of Leo A's mass:

$$M_{proj} = \frac{f}{G(N-\alpha)} \sum_{i=1}^{N} V_{z,i}^2 R_{\perp,i} \qquad (1)$$

where G is the gravitational constant, N is the number of stars, α is an empirical correction to the center of mass (Heisler et al. use $\alpha = 1.5$), V_z is the velocity relative to the mean, $R_\perp$ is the projected separation from the center of the galaxy, and f is a constant that depends on the eccentricity of the stellar orbits. For purely isotropic orbits $f = 32/\pi$, while for purely radial orbits $f = 64/\pi$. Using the velocities and positions in Table 1, Leo A has a kinematic mass of $5.3 \pm 1.3 \times 10^7$ $M_\odot$ for purely isotropic orbits and $10.6 \pm 2.6 \times 10^7$ $M_\odot$ for purely radial orbits. Heisler et al. prefer using the smaller mass derived from isotropic orbits, but for purposes of discussion, we will assume that Leo A's mass is the average of the two projected mass estimates: 8×10^7 $M_\odot$. This mass is derived from objects inside a radius of $2' = 500$ pc.

By comparison, Vansevičius et al. (2004) estimate that Leo A's stellar mass is $M_{stars} = 4 \pm 2 \times 10^6$ $M_\odot$, consistent with the galaxy's optical luminosity. More recently, Lee et al. (2006) use *Spitzer* 4.5μm imaging to estimate that Leo A's total stellar mass is $M_{stars} = 0.8 \times 10^6$ $M_\odot$ with an uncertainty of 0.5 dex. These stellar mass estimates are factors of 20 - 100 times smaller than our kinematic mass estimate.

Leo A's total V-band luminosity is $M_V = -11.7$, which comes from the apparent magnitude $V_{tot} = 12.8 \pm 0.2$ (Mateo 1998) and the distance modulus $(m - M)_0 = 24.51 \pm 0.12$ (Dolphin et al. 2002). Assuming the Sun has $M_{V,\odot} = +4.8$, Leo A's total luminosity in solar units

TABLE 1
LEO A BLUE PLUME OBJECTS

RA J2000	Dec J2000	type	v_{helio} km s^{-1}	g' mag	$(u' - g')_0$ mag	$(g' - r')_0$ mag
9:59:15.124	30:44:10.40	B	23.0 ± 2.5	19.896	0.761	-0.279
9:59:16.940	30:43:48.22	B	21.7 ± 5.2	19.050	-0.021	-0.353
9:59:20.223	30:43:52.71	B	34.0 ± 2.8	19.435	0.458	-0.375
9:59:23.220	30:45:06.23	B	7.4 ± 3.8	20.026	0.584	-0.347
9:59:24.909	30:44:36.69	B	30.9 ± 3.4	19.797	1.004	-0.257
9:59:25.980	30:46:10.44	B	9.5 ± 5.0	20.964	0.652	-0.397
9:59:26.351	30:45:26.09	B	37.6 ± 2.3	19.131	0.412	-0.300
9:59:27.058	30:45:38.79	B	21.9 ± 4.7	20.267	0.982	-0.388
9:59:27.326	30:45:44.69	B	7.6 ± 4.9	20.661	1.082	-0.420
9:59:27.532	30:44:57.75	HII	30.0 ± 3.6	19.984	-0.238	-0.607
9:59:32.129	30:43:48.55	B	22.0 ± 2.6	20.471	0.383	-0.360
9:59:33.320	30:44:39.21	HII	22.2 ± 4.2	19.520	-0.288	-0.252

is 4×10^6 $L_\odot$. Thus the mass-to-light ratio of Leo A is $M/L_{tot} = 20 \pm 6$ $M_\odot/L_\odot$ for a mass of 8×10^7 $M_\odot$. Because our spectroscopic targets do not sample the full extent of Leo A, this mass-to-light ratio is a lower limit to Leo A's true mass-to-light ratio.

A mass-to-light ratio of 20 suggests that Leo A is dominated by dark matter. Young & Lo (1996) reach the opposite conclusion from their H I velocity dispersion, but their result is explained by the revision of Leo A's distance from 2.2 Mpc to 800 kpc. Leo A's total H I mass within $a = 8'$ is $M_{HI} = 1.0 \pm 0.2 \times 10^7$ $M_\odot$ (Allsopp 1978; Young & Lo 1996) at a distance of 800 kpc. The gas mass includes the 10% correction for helium gas. Thus baryonic matter – stars plus gas – accounts for at most $\sim$20% of Leo A's total mass.

4. DISCUSSION AND CONCLUSIONS

We have obtained spectroscopy for twelve blue plume objects in the central 2′ of Leo A. Ten of these objects are young B supergiants. We measure a stellar velocity dispersion of $\sigma = 9.3 \pm 1.3$ km s^{-1}, identical to Leo A's H I gas dispersion (Young & Lo 1996). From this we estimate a projected mass of $8 \pm 2.7 \times 10^7$ $M_\odot$, which implies that Leo A's mass is at least $\sim$80% dark matter.

Dwarf galaxies are thought to be the smallest bodies containing dynamically significant amounts of dark matter, and so it is interesting to place Leo A in the context of cosmological simulations. Evrard et al. (2007) show that the velocity dispersion of dark matter halos follow a tight correlation with total mass, $\sigma_{DM} = (1084 \pm 13\ \mathrm{kms}^{-1})(h(z)M_{200}/10^{15}\ M_\odot)^{0.3359 \pm 0.0045}$, where M_{200} is the mass within a sphere with mean interior density 200 times the critical density. Leo A's mass, 8×10^7 $M_\odot$, would fill such a sphere with a radius of $r_{200} = 9$ kpc. The halo virial relation is derived from $\sim 10^{15}$ $M_\odot$ dark matter halos, but Evrard et al. show it is valid down to $\sim 10^{10}$ $M_\odot$ halos. If we simply equate Leo A's mass to M_{200}, the halo virial relation predicts $\sigma_{DM} = 4$ km s^{-1} for $h(z) = 0.70$. This prediction is less than half of the observed velocity dispersion. One possible explanation for the discrepancy is that Leo A has not reached dynamical equilibrium, and thus its velocity dispersion is inflated (Young & Lo 1996). Or, perhaps the discrepancy suggests that dwarfs like Leo A experience a different evolutionary path than a purely hierarchical growth of dark matter halos.

Remarkably, Leo A's stellar velocity dispersion is very
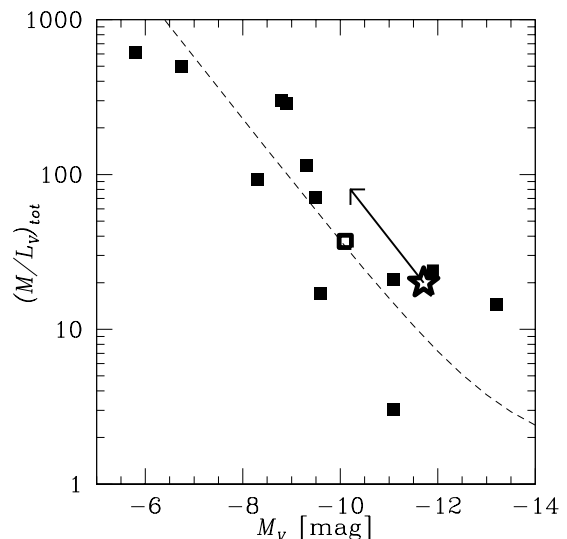

FIG. 5.— Mass-to-light ratio of Local Group dSph galaxies with masses determined from central velocity dispersions (*solid squares*), adapted from Mateo (1998) and Koch et al. (2007). The dashed line is the $(M/L)_{tot}$ relation for a galaxy in a dark matter halo of constant mass $3 \times 10^7 M_\odot$. We estimate $M/L = 20 \pm 6$ for Leo A (*star*), which falls near the fixed halo mass relation. The arrow indicates what happens if Leo A stops forming stars and fades to a dSph-like color. The Phoenix transition dwarf (*open square*) also agrees with the fixed halo mass relation.

similar to that of Local Group dwarf spheroidals (dSphs), which have central velocity dispersions of 8 to 10 km s^{-1} (Mateo 1998). One explanation for the common central velocity dispersion is that all Local Group dwarfs are enclosed in dark matter halos of similar total mass (Mateo et al. 1993). Galaxies with smaller velocity dispersions (total mass $\lesssim 10^8$ $M_\odot$) are possibly re-ionized and thus never form stars (e.g. Navarro & Steinmetz 1997). If this picture is correct, then the total mass to light ratio of a dwarf is a function of its luminosity $(M/L)_{tot} = M_{DM}/L + (M/L)_*$, where M_{DM} is the fixed dark matter halo mass, L is the total V-band luminosity, and $(M/L)_*$ is the stellar mass to light ratio.

In Figure 5 we plot the $(M/L)_{tot}$ versus V-band luminosity for Local Group dSphs with central velocity dispersion measurements. We note that Leo A has a central velocity dispersion and no observed rotation, thus its dynamical mass is directly comparable with dSphs. Dwarf irregulars have masses deter-

mined from rotation and are not directly comparable. We base Figure 5 on the Koch et al. (2007) version of Mateo (1998)'s plot. The solid squares are And II (Côté et al. 1999), And IX (Chapman et al. 2005), Boötes (Belokurov et al. 2006; Muñoz et al. 2006), Carina and Sextans (Wilkinson et al. 2006), Draco and Ursa Minor (Wilkinson et al. 2004), Fornax (Wang et al. 2005), Leo I (Koch et al. 2007), Leo II and Sculptor (Mateo 1998), and Ursa Major (Willman et al. 2005; Kleyna et al. 2005). The dashed line shows the $(M/L)_{tot}$ relation for a fixed dark matter halo mass $M_{DM} = 3 \times 10^7 \ M_\odot$ and stellar $(M/L)_* = 1.5 \ M_\odot/L_\odot$ (Koch et al. 2007). Leo A, plotted as a star, falls very near the fixed halo mass relation for dSphs.

However, Leo A's stellar population is quite different from that of the dSphs. Integrated colors provide a quantitative measure of the difference: Leo A has $(B-V) = 0.15$, systematically bluer than the average dSph with $(B-V) = 0.8 \pm 0.25$ (Mateo 1998). As its stellar population ages, Leo A's luminosity will decrease and its mass to light ratio will increase. We estimate this change using Starburst99 (Leitherer et al. 1999; Vázquez & Leitherer 2005) with $Z = 0.0004$ Padova tracks. We find that in a couple of Gyr, assuming Leo A has no further star formation, it will reach $(B-V) = 0.8$ and will have faded ~ 1.5 magnitudes in M_V. We indicate this evolution with the arrow in Figure 5. Leo A still falls well within the observed scatter around the $(M/L)_{tot}$ relation.

Comparing Leo A with "transition dwarfs" may be more fair than comparing with dSphs. Transition dwarfs have old stellar populations like dSphs, but also contain gas and young stars like Leo A. A central velocity dispersion is available for the Phoenix transition dwarf (Mateo 1998) (the open square in Figure 5), which places it squarely on the $(M/L)_{tot}$ relation. Thus, despite their different star formation histories, Leo A, Phoenix, and the dSphs appear to share remarkably similar kinematics and dark matter halo mass.

If transition dwarfs represent the stage between gas-rich dwarf irregulars and gas-poor dSphs, this evolution must involve some amount of galaxy interaction. Most dSphs in the Local Group are located near the major spirals, so the dSphs' lack of gas and young stars likely results from repeated gravitational and/or hydrodynamic interactions with the spirals. In a comprehensive study of minor galaxy interactions in the SDSS, Freedman Woods & Geller (2007) find that the lowest luminosity galaxies in close pairs experience the largest fractional boosts in their specific star formation rates. Perhaps Leo A's episodic star formation history is a history of its interactions with objects in the Local Group.

One clue to the evolution of transition dwarfs in the Local Group may come from comparison of the rotation velocity and central velocity dispersion. A wide variety of studies demonstrate the relation between these kinematic measures and the formation history of galaxies (e.g. Pizzella et al. 2005; Jesseit et al. 2005; de Rijcke et al. 2005; De Rijcke et al. 2006). Multi-slit spectrographs can now provide radial velocities for hundreds of stars in nearby dwarfs, making such studies possible for the first time.

REFERENCES

Adelman-McCarthy, J. K. et al. 2007, ApJS, in press
Allsopp, N. J. 1978, MNRAS, 184, 397
Bahcall, J. N. & Tremaine, S. 1981, ApJ, 244, 805
Belokurov, V. et al. 2006, ApJ, 647, L111
Brown, W. R., Geller, M. J., Kenyon, S. J., & Kurtz, M. J. 2006, ApJ, 647, 303
Brown, W. R., Geller, M. J., Kenyon, S. J., Kurtz, M. J., & Bromley, B. C. 2007, ApJ, 660, 311
Chapman, S. C., Ibata, R., Lewis, G. F., Ferguson, A. M. N., Irwin, M., McConnachie, A., & Tanvir, N. 2005, ApJ, 632, L87
Cole, A. et al. 2007, pre-print astro-ph/0702646
Corbally, C. J. & Garrison, R. F. 1984, in The MK Process and Stellar Classification, ed. R. F. Garrison, 277
Côté, P., Mateo, M., Olszewski, E. W., & Cook, K. H. 1999, ApJ, 526, 147
de Rijcke, S., Michielsen, D., Dejonghe, H., Zeilinger, W. W., & Hau, G. K. T. 2005, A&A, 438, 491
De Rijcke, S., Prugniel, P., Simien, F., & Dejonghe, H. 2006, MNRAS, 369, 1321
Demers, S., Kibblewhite, E. J., Irwin, M. J., Bunclark, P. S., & Bridgeland, M. T. 1984, AJ, 89, 1160
Dolphin, A. E., Saha, A., Claver, J., Skillman, E. D., Cole, A. A., Gallagher, J. S., Tolstoy, E., Dohm-Palmer, R. C., & Mateo, M. 2002, AJ, 123, 3154
Evans, D. S. 1967, in IAU Symp. 30: Determination of Radial Velocities and their Applications, ed. A. H. Batten & J. F. Heard, 57
Evrard, A. E. et al. 2007, preprint astro-ph/0702241

Freedman Woods, D. & Geller, M. J. 2007, AJ, submitted
Gray, R. O., Corbally, C. J., Garrison, R. F., McFadden, M. T., & Robinson, P. E. 2003, AJ, 126, 2048
Heisler, J., Tremaine, S., & Bahcall, J. N. 1985, ApJ, 298, 8
Jesseit, R., Naab, T., & Burkert, A. 2005, MNRAS, 360, 1185
Kleyna, J. T., Wilkinson, M. I., Evans, N. W., & Gilmore, G. 2005, ApJ, 630, L141
Koch, A., Wilkinson, M. I., Kleyna, J. T., Gilmore, G. F., Grebel, E. K., Mackey, A. D., Evans, N. W., & Wyse, R. F. G. 2007, ApJ, 657, 241
Kurtz, M. J. & Mink, D. J. 1998, PASP, 110, 934
Lee, H., Skillman, E. D., Cannon, J. M., Jackson, D. C., Gehrz, R. D., Polomski, E. F., & Woodward, C. E. 2006, ApJ, 647, 970
Leitherer, C., Schaerer, D., Goldader, J. D., Delgado, R. M. G., Robert, C., Kune, D. F., de Mello, D. F., Devost, D., & Heckman, T. M. 1999, ApJS, 123, 3
Lo, K. Y., Sargent, W. L. W., & Young, K. 1993, AJ, 106, 507
Mateo, M., Olszewski, E. W., Pryor, C., Welch, D. L., & Fischer, P. 1993, AJ, 105, 510
Mateo, M. L. 1998, ARA&A, 36, 435
Muñoz, R. R., Carlin, J. L., Frinchaboy, P. M., Nidever, D. L., Majewski, S. R., & Patterson, R. J. 2006, ApJ, 650, L51
Navarro, J. F. & Steinmetz, M. 1997, ApJ, 478, 13
Pizzella, A., Corsini, E. M., Dalla Bontà, E., Sarzi, M., Coccato, L., & Bertola, F. 2005, ApJ, 631, 785
Sandage, A. 1986, AJ, 91, 496
Schaller, G., Schaerer, D., Meynet, G., & Maeder, A. 1992, A&AS, 96, 269

Schlegel, D. J., Finkbeiner, D. P., & Davis, M. 1998, ApJ, 500, 525
Schulte-Ladbeck, R. E., Hopp, U., Drozdovsky, I. O., Greggio, L., & Crone, M. M. 2002, AJ, 124, 896
Skillman, E. D., Kennicutt, R. C., & Hodge, P. W. 1989, ApJ, 347, 875
Tolstoy, E. 1996, ApJ, 462, 684
Tolstoy, E. et al. 1998, AJ, 116, 1244
van Zee, L., Skillman, E. D., & Haynes, M. P. 2006, ApJ, 637, 269
Vansevičius, V. et al. 2004, ApJ, 611, L93
Vázquez, G. A. & Leitherer, C. 2005, ApJ, 621, 695
Wang, X., Woodroofe, M., Walker, M. G., Mateo, M., & Olszewski, E. 2005, ApJ, 626, 145

Wilkinson, M. I., Kleyna, J. T., Evans, N. W., Gilmore, G. F., Irwin, M. J., & Grebel, E. K. 2004, ApJ, 611, L21
Wilkinson, M. I., Kleyna, J. T., Wyn Evans, N., Gilmore, G. F., Read, J. I., Koch, A., Grebel, E. K., & Irwin, M. J. 2006, in EAS Publications Series, ed. G. A. Mamon, F. Combes, C. Deffayet, & B. Fort, 105–112
Willman, B. et al. 2005, ApJ, 626, L85
Young, L. M. & Lo, K. Y. 1996, ApJ, 462, 203
Zwicky, I. F. 1942, Phys. Rev., 61, 489